By Ping Sun, Rui Shan, and Shuoyu Wang

The demand for walking training robots has increased owing to a serious shortage of rehabilitation physiotherapists. However, the intelligence level of existing rehabilitation training robots is low; these robots cannot realize a direct switch between passive and active training, which makes rehabilitees lack interest in training and deteriorates the effect of rehabilitation training. In this study, a rehabilitation gait training robot is developed in line with the characteristics of human omnidirectional walking. The proposed robot uses a suitable control algorithm to accurately follow the exercise programs prescribed by physical therapists and can realize fine practice results. The novelty of the robot is that passive and active training can be directly and gently switched during walking. The passive training stage has a velocity restriction safety function, whereas the active training stage has a velocity decision function. The purpose of this design is to avoid sudden changes in the robot velocity during the passive training

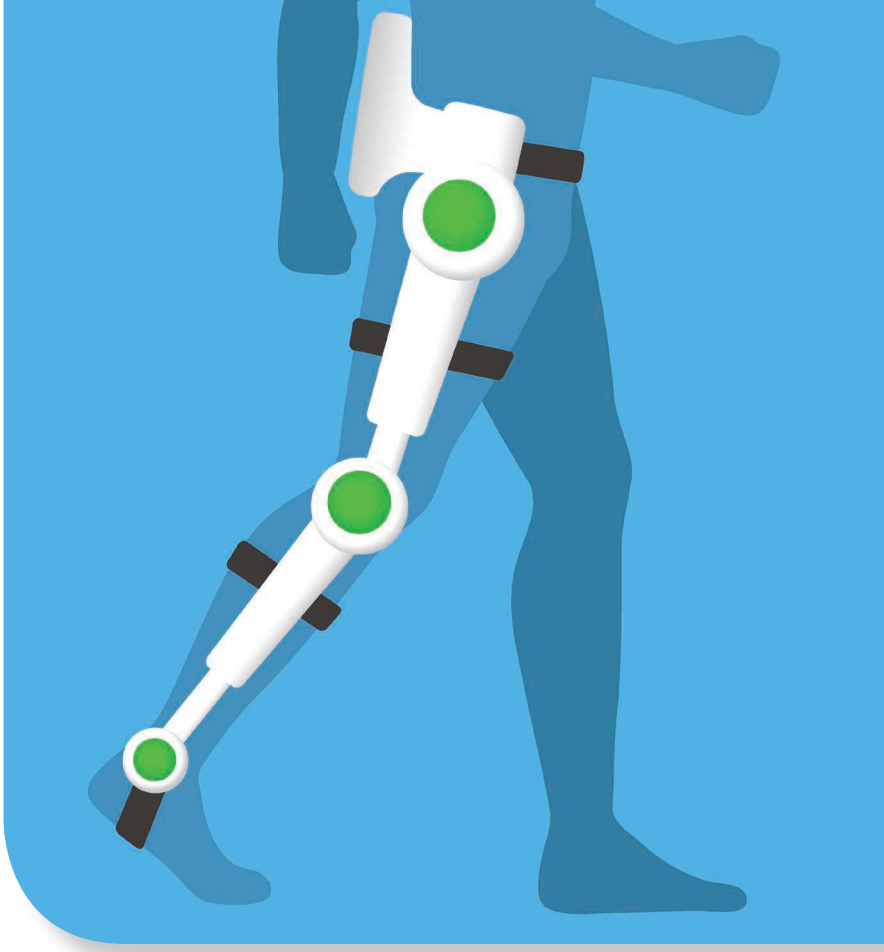

An Intelligent Rehabilitation Robot With Passive and Active Direct Switching Training

Improving Intelligence and Security of Human–Robot Interaction Systems

Digital Object Identifier 10.1109/MRA.2022.3228490
Date of current version: 28 December 2022

1070-9932/22©2022IEEE

stage and to guarantee the coordination of the human–robot velocity in the active training stage. Comparative simulation analyses and experimental results show that the proposed passive and active direct switching training improves the intelligence and security of rehabilitation robot.

INTRODUCTION

As prototypical physical human–robot interaction systems, rehabilitation training robots have been developed that help rehabilitees with walking disorders by tracking the training trajectories preset by rehabilitation physiotherapists. Walking exercises can be performed to enhance the leg muscle strength and balance ability of rehabilitees, so that their independent walking function can be gradually restored. A variety of training robots have been developed to address the problems of aging societies, such as gait exoskeleton robots [1] and ankle rehabilitation robots [2]. With the help of rehabilitation robots, rehabilitees with walking disabilities can realize good rehabilitation outcomes through repeated walking exercises.

> “THE NOVELTY OF THE ROBOT IS THAT PASSIVE AND ACTIVE TRAINING CAN BE DIRECTLY AND GENTLY SWITCHED DURING WALKING.”

In recent years, the number of stroke rehabilitees in China has increased at an annual growth rate of 10% [3]. However, there is a serious shortage of physiotherapists and medical resources in China, which increases the workload of physiotherapists and deteriorates the effectiveness of rehabilitation. Thus, the development of rehabilitation training robots not only decreases the work pressure of physiotherapists but also enables rehabilitees to receive timely rehabilitation training. Since the leg strength of rehabilitees is weak in the early training stage, it is often necessary to passively track the training trajectories specified by doctors. Passive training robots have been developed, such as lower-limb rehabilitation robots with trajectory tracking, that are suitable for the passive training of rehabilitees with paralyzed or weak limbs [4]. A rehabilitation robot driven by a multifilament was designed based on a motion model and a system elbow joint model [5]. These robots have only a passive training mode and are only suitable for the initial rehabilitation training of rehabilitees. With the enhancement of the rehabilitees' motor function, these robots cannot actively participate in training.

In fact, there are some research results on the active training of rehabilitation training robots, such as ankle rehabilitation robots, where the subjects are required to accomplish a task within a predefined time by rotating the ankle joints with the assistance of the robots based on visual or auditory instructions [6]. Additionally, a robot-assisted treadmill-based exoskeleton gait training program with an active assistant protocol robot was developed. This program uses haptic feedback to enhance resist motion rather than pointing the upper extremity ankle toward or away from the path [7]. A particle-filtered interface function was proposed to estimate and predict the locations of the rehabilitee's lower limbs and body, thereby realizing the natural and smooth active movement of the Japan Advanced Institute of Science and Technology robotic walker [8]. Active and passive hybrid training modes are also available. In [9], an end-effector typed hybrid walking rehabilitation robot with three modes was proposed to help rehabilitees in different rehabilitation stages, and the three modes were passive, assisted active, and active. Further, a rehabilitation robot named DDgo pro was developed; its passive mode let the robot fully guide a normal walking pattern, and the active assisted mode performed rehabilitation training for a long time while receiving muscle assistance from the robot [10]. The above robots have an active training mode or passive and active mixed training modes. However, when the robot is in the passive training mode, the current motion should be stopped to switch to the active training mode. For rehabilitees with weak leg strength, the upper limbs need to support their body weight, and it is very difficult to switch the training modes back and forth.

Additionally, many commercial rehabilitation robots have advanced significantly, including the walking balance robots Erigo, Lokomat, and Andago [11] and wearable robot Hybrid Assistive Limb (HAL) [12]. To achieve the rehabilitation training of the leg muscles, Erigo and Lokomat, two robots for walking balance, adopted the training modes of a pedal and a treadmill, respectively. Due to the fact that walking is essentially a movement on the ground, the rehabilitation robots mentioned above are unable to simulate actual walking training with friction between the feet and the ground. A technique that shows promise is gait rehabilitation training while receiving partial bodyweight support from a robot [13]. Instead of switching directly from passive to active training mode, the Andago device that enables bodyweight support while walking over ground has three training modes: rehabilitee following, straight line, and manual. HAL can only help people with disabilities whose lower limbs cannot regain the ability to walk using bioelectric potential signals to move in accordance with the wearer's intention to maintain physical function.

Rehabilitative walking robots need to track training trajectories specified by doctors. Researchers have proposed various tracking control methods, such as fuzzy sliding mode control in rehabilitation environments [14], robust iterative feedback tuning control for repetitive ankle training [15], and neural network control of rehabilitation robots using state and output feedback [16]. However, these methods, whether in the passive or active training mode, ignore the impact of uncertain environments of human–robot movements on the tracking performance, resulting in unsatisfactory tracking accuracy. Moreover, there are no safety constraints with regard to the velocity of human–robot movements. When the robot's velocity is mutated, the rehabilitee safety is seriously

threatened. Therefore, the control technique for ensuring the safe movement of human–robot systems is a key factor in the design of rehabilitation robots.

This study discusses the development of a rehabilitation robot with passive and active direct switching training [rehabilitation robot direct switching (RRDS)] [17]. Only the passive training mode of the rehabilitee following robot movement was examined in [17], and the mode transitioning to active training following the development of the rehabilitee's leg strength was not taken into account compared with other walking training robots. The main features of RRDS are as follows:

1) The passive and active training modes of the robot can be directly switched in line with the walking characteristics of people with dysfunctional walking.
2) A stochastic configuration network (SCN) with a simple structure is used to estimate the uncertainty, and the hidden layer nodes are randomly configured to accurately depict human–robot motion environments.
3) A novel passive and active direct switching control method is proposed, and passive constraints and active decision-making concerning movement velocity can be realized.

Several simulation comparative analyses and experimental studies have been performed on RRDS.

STRUCTURE DESCRIPTION OF THE RRDS

The RRDS is a rehabilitation walking training robot designed for rehabilitees with lower-extremity disorders. The robot stores many paths as desired movement paths after the physiotherapist creates various training paths based on the rehabilitee's capacity for walking. To help the rehabilitee walk more easily and address the shortage of physiotherapists for rehabilitation, the robot typically needs to follow a predetermined path. The overall structure consists of a touch panel, an armrest, ultrasonic sensors, omnidirectional wheels, and a height-adjustable main body bracket, as shown in Figure 1.

- The touch panel, as shown in Figure 1(a), can be used to select the training mode of the robot and stop the robot in the case of an emergency. In the rehabilitation training process, a rehabilitee can walk in multiple directions, such as forward and backward, or turn according to the doctor's training program. Moreover, training can be stopped immediately when an emergency is encountered. The RRDS can help in independent rehabilitation training without the need for doctor on-site care.
- An armrest, as shown in Figure 1(b), is used to support the rehabilitee's body. In walking training, rehabilitees should place their forearms on the armrest to reduce the pressure on the lower limbs. Pressure sensors were placed under the armrest to obtain the pressure information of the forearm on the RRDS.
- When the ultrasonic sensor, as shown in Figure 1(c), is running, it sends ultrasonic information to the surroundings and feeds back the motion environment to a certain extent. It is also used to avoid obstacles in the case of collision risk.
- As shown in Figure 1(d), the omniwheel is a prominent structural feature of the RRDS design. There are four omniwheels, each of which is independently driven by a dc motor. Combined with the appropriate tracking control

FIGURE 1. RRDS structure and walking training. (a) Touch panel, (b) armrest, (c) ultrasonic sensor, (d) omniwheel, and (e) safety seat.

method, the four omniwheels allow the RRDS to move in any direction, even in a confined space, and they can also assist the RRDS in rehabilitation through walking exercises.

- The safety seat, as shown in Figure 1(e), is connected to the force sensor and is placed under the buttocks of the rehabilitee; it is used to deal with the occurrence of unexpected situations. The rehabilitee who is about to fall down will sit on the safety seat first due to insufficient leg strength. At this point, the safety seat's sensor can detect pressure, causing the RRDS to stop moving gradually to keep the robot performing safely and prevent the rehabilitee from falling.

> "THEREFORE, THE CONTROL TECHNIQUE FOR ENSURING THE SAFE MOVEMENT OF HUMAN–ROBOT SYSTEMS IS A KEY FACTOR IN THE DESIGN OF REHABILITATION ROBOTS."

During the rehabilitation training process, the walking ability of the rehabilitee is relatively weak at the beginning. Typically, the rehabilitee must move by mimicking the velocity of the RRDS, which is passive training. The rehabilitee can walk at the velocity of his own willingness to engage in the walking movement, which is active training, as his walking ability improves. To help the rehabilitee train and develop its intelligence, the RRDS must now determine the rehabilitee's walking velocity and decide how to change its own velocity to keep up with the rehabilitee. Regardless of whether the rehabilitee is receiving passive or active training, RRDS must undoubtedly follow the training trajectory recommended by the physiotherapist to realize tracking motion.

Several studies have been conducted on rehabilitation robots with passive and active hybrid training. However, in most of the proposed models, the robot needs to be set to stop the current state of motion when switching the training mode, and then it should be restarted to enter the next training mode. However, changing the training modes back and forth by stopping is neither comfortable nor convenient. Moreover, the legs of rehabilitees are usually weak, and the affected limbs may be injured because of the movement inertia of the robot. If a robot can directly enter the active training stage from the passive training stage, it can align with the characteristics necessary for walking rehabilitation training.

CONTROL METHOD FOR PASSIVE AND ACTIVE DIRECT SWITCHING TRAINING

RRDS DYNAMICS MODEL WITH HUMAN–ROBOT UNCERTAIN ENVIRONMENTS

The RRDS has four omnidirectional wheels driven by dc motors. Older people or people with lower-limb disabilities can be included in rehabilitation training. The structural coordinates of the robot are shown in Figure 2.

Here $\Sigma(x, O, y)$ is the global coordinate system, and $\Sigma(x', C, y')$ is the translation coordinate system. v is the motion velocity of the robot, and v_ν is the velocity of each wheel. α is the angle between v and the x' axis, and β is the angle between r_0 and the x' axis. f_ν is the control input force for each driven wheel, L is the distance between the center of the RRDS and each wheel, l_ν is the distance between the center of gravity of the RRDS and the center of each wheel, and r_0 is the distance between the center of gravity of the RRDS and the center C, $\nu = 1, 2, 3, 4$.

During actual training processes, rehabilitation robots need to track the paths specified by doctors. Since the postures and leg strengths of the rehabilitees are different, rehabilitation robots encounter uncertain environments. If the uncertain environments of a human–robot cooperative motion cannot be solved, the RRDS cannot obtain accurate trajectory tracking. Therefore, it is important to construct a dynamic model with uncertain environments for rehabilitation robots.

The dynamic model of RRDS is described as follows [17]:

$$M_1\ddot{X}(t) + M_2\dot{X}(t) = B(\theta)u(t) \tag{1}$$

with the following definitions:

- M_1, M_2, and $B(\theta)$ denote the coefficient matrices, and their specific meanings are as in [17].
- $X(t)$ is the actual motion trajectory of the RRDS, and $X(t) = [x(t) \;\; y(t) \;\; \theta(t)]^T$.
- $u(t)$ is the control input force, and $u(t) = [f_1 \;\; f_2 \;\; f_3 \;\; f_4]^T$.
- θ is the angle between the horizontal axis and the line connecting the center of the robot and the first wheel. That is, $\theta_1 = \theta$. As can be observed from the robot structure, $\theta_2 = \theta + \pi/2, \theta_3 = \theta + \pi$, and $\theta_4 = \theta + 3\pi/2$.

The physical quantities affected by the changes in the rehabilitee's pose are separated from system model (1); that is, $M_1 = M_a + \Delta M_a$. Thus, the RRDS dynamic model with uncertain environments can be established as follows:

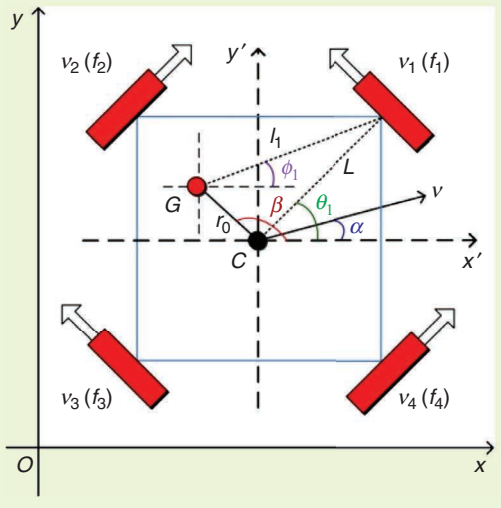

FIGURE 2. Structure coordinates of the RRDS.

$$\ddot{X}(t) = M_a^{-1} B(\theta) u(t) + \xi(t). \tag{2}$$

Here

$$M_a = \begin{bmatrix} M+m & 0 & 0 \\ 0 & M+m & 0 \\ 0 & 0 & I_0 \end{bmatrix}, \Delta M_a = \begin{bmatrix} 0 & 0 & p(M+m) \\ 0 & 0 & q(M+m) \\ 0 & 0 & mr_0^2 \end{bmatrix}$$

where $\xi(t) = -M_a^{-1}(\Delta M_a \ddot{X}(t) + M_2 \dot{X}(t))$ constitutes the uncertain environments of the RRDS, which differs based on the rehabilitee. M is the mass of the RRDS, and m is the rehabilitee's mass.

ESTIMATION OF HUMAN–ROBOT UNCERTAIN ENVIRONMENTS

The SCN method was used to build a network identification system model of human–robot uncertain environments, and the motion trajectory and velocity were used as the network inputs. The human–robot uncertainty environments were obtained by the continuous and random configuration of the hidden layer node. The workflow is summarized as follows:

- The motion trajectory and velocity $x(t) = [X(t), \dot{X}(t)]^T$ of the RRDS are used as the network input layer of the SCN, which is connected to the hidden layer through the weight ω and threshold b, and the output $G(x(t))$ of the hidden layer is obtained using the Gaussian function. Here $\omega = [\omega_1, \omega_2, \ldots, \omega_Q]^T, b = [b_1, b_2, \ldots, b_Q]^T, G(x(t)) = [g_1(\omega_1 x(t) + b_1), \ldots, g_Q(\omega_Q x(t) + b_Q)]^T$.
- The SCN hidden layer is connected to the output layer through the weight $\hat{\beta}$, and the network output $\hat{\xi}_Q(t)$ of the system uncertain environment is $\hat{\xi}_Q(t) = \hat{\beta}^T G(x(t))$, $\hat{\beta}^T = [\hat{\beta}_1, \hat{\beta}_2, \ldots, \hat{\beta}_Q]$.
- According to the human–robot uncertain environment error $\varepsilon_{Q-1} = \xi(t) - \hat{\xi}_{Q-1}(t)$ obtained when the number of hidden layer nodes is $Q-1$, the parameters of the Qth hidden layer node are randomly configured to satisfy $\delta_Q > 0$, and the expression form of δ_Q is as follows:

$$\delta_Q = \frac{((\varepsilon_{Q-1})^T g_Q(\omega_L x_k(t) + b_Q))^2}{(g_Q(\omega_Q x_k(t) + b_Q))^T g_L(\omega_Q x_k(t) + b_Q) - (1 - r - \mu_Q)(\varepsilon_{Q-1})^T \varepsilon_{Q-1}} \tag{3}$$

where the parameters $0 < r < 1$ and $\{\mu_Q\}$ are nonnegative real number sequences, $\mu_Q \le 1 - r$, and $\lim_{Q \to +\infty} \mu_Q = 0$. As the number of randomly configured hidden layer nodes continues to increase until $\lim_{Q \to \infty} \varepsilon_Q = 0$, the human–robot uncertain environment identification $\hat{\xi}_Q(t) = \xi(t)$ of the RRDS system can be realized. The SCN structure is as shown in Figure 3.

As shown in Figure 3, the actual position and velocity of the robot were used as inputs for the neural network. Moreover, the implicit layer node parameters were constantly randomly configured, and under the supervision mechanism (3), the estimation of the human–robot uncertain environments was obtained.

PASSIVE AND ACTIVE DIRECT SWITCHING TRAINING

PASSIVE TRAINING

SAFE VELOCITY PREDICTION CONSTRAINT

In the passive training mode, owing to the uncertain environments of human–robot coordinated movements, sudden velocity changes are inevitable, and they can seriously threaten the safety of the rehabilitee. Therefore, the robot velocity must have limitations. Here we used the kinematic model of the RRDS to propose a model prediction constraint method to limit the actual velocity of each wheel. The kinematic model of the RRDS is described as $V(t) = K_G(t)\dot{X}(t)$, where

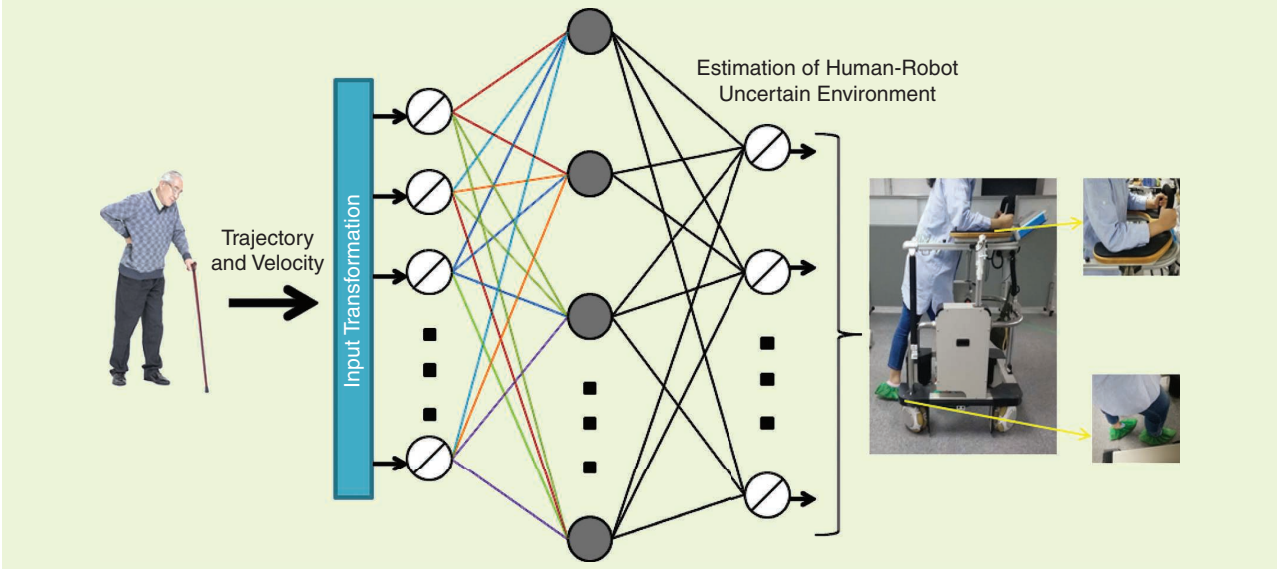

FIGURE 3. SCN structure.

$$K_G(t)=\begin{bmatrix}-\sin\theta & \cos\theta & L\\ \cos\theta & \sin\theta & -L\\ -\sin\theta & \cos\theta & -L\\ \cos\theta & \sin\theta & L\end{bmatrix}.$$

It should be noted that the discretized model in the kinematic model can be written as follows given the system state $X(t)$ by expressing the output as $Y(t)=X(t)$. Using the nonlinear feedforward difference method and rewriting the velocity input $V(t)$ in incremental form,

$$\begin{cases}X(k+1)=AX(k)+BV(k)\\ V(k)=V(k-1)+\Delta V(k)\\ Y(k)=\dot{X}(k)=BV(k)\end{cases}\tag{4}$$

where $V(k-1)$ is the velocity input of the system in the previous moment and $\Delta V(k)$ is the velocity increment in the current moment. The matrix $A=I_3$, and I_3 is the identity matrix. $B=T\cdot K_N(t)$ is the input matrix, $K_N(t)=(K_G(t)\,K_G^T(t))^{-1}$ $K_G^T(t)$ is the pseudo-inverse of $K_G(t)$, and T is the sampling period.

Here N is the prediction time horizon, and NC is the control time horizon. To constrain the actual velocity of the RRDS, the following constraints were established for the motion and input velocities of each wheel:

$$\begin{cases}\bar{\dot{X}}_{\min}\le\bar{\dot{X}}\le\bar{\dot{X}}_{\max}\\ \bar{V}_{\min}\le\bar{V}\le\bar{V}_{\max}\end{cases}\tag{5}$$

where $\bar{V}$ and $\bar{\dot{X}}$ denote the predicted velocity input at future time steps from k to $k+N_C-1$ and the predicted actual motion velocity at future time steps from k to $k+N-1$, respectively. The upper and lower limits of the system input are $\bar{V}_{\max}$ and $\bar{V}_{\min}$, respectively, where $\bar{V}_{\max}=-\bar{V}_{\min}$. The upper and lower limits of motion velocity are $\bar{\dot{X}}_{\max}$ and $\bar{\dot{X}}_{\min}$, respectively, where $\bar{\dot{X}}_{\max}=-\bar{\dot{X}}_{\min}$. According to (4), the motion velocity of the RRDS is given by $\bar{\dot{X}}=\Gamma V(k-1)+\Theta\Delta\bar{V}$. Here $\Delta\bar{V}=[\Delta V^T(k\,|\,k),\Delta V^T(k+1\,|\,k),\ldots,\Delta V^T(k+N_C-1\,|\,k)]^T,\Gamma=F_qZ_0,\Theta=F_qZ_1,Z_0=[I_4,I_4,\cdots,I_4]^T_N$,

$$Z_1=\begin{bmatrix}I_4 & 0 & \cdots & 0\\ I_4 & I_4 & \cdots & 0\\ \vdots & \vdots & \ddots & \vdots\\ I_4 & I_4 & \cdots & I_4\end{bmatrix}_N,$$

$$F_q=\begin{bmatrix}F(k) & 0 & \cdots & 0\\ 0 & F(k+1) & \cdots & 0\\ \vdots & \vdots & \ddots & \vdots\\ 0 & 0 & \cdots & F(k+N-1)\end{bmatrix}$$

where Z_1 and F_q are the decomposition matrices of the coefficients Γ and Θ in the predictive velocity model, respectively, and $F(k+\omega),\omega=0,1\ldots N-1$ is the input coefficient matrix corresponding to the RRDS system for future time steps from k to $k+N-1$. By substituting the motion velocity of the RRDS into (5), the constraint for the increment in the predicted time domain can be obtained as follows:

$$\Theta_0\Delta\bar{V}\le d.\tag{6}$$

Here $\Theta_0=[-\Theta^T\Theta^T-Z_1^TZ_1^T]^T,d=[-d_{1\min}^Td_{1\max}^T-d_{2\min}^T$ $d_{2\max}^T]^T,d_{1\min}=\bar{\dot{X}}_{\min}-\Gamma V(k-1),d_{1\max}=\bar{\dot{X}}_{\max}-\Gamma V(k-1),$ $d_{2\min}=\bar{V}_{\min}-Z_0V(k-1),d_{2\max}=\bar{V}_{\max}-Z_0V(k-1)$.

To minimize the actual velocity tracking error of the robot and the velocity input increment of each wheel, the objective function can be established as $J=\min(\bar{\dot{X}}-\bar{\dot{X}}_d)^T$ $\Pi(\bar{\dot{X}}-\bar{\dot{X}}_d)+\Delta\bar{V}^T\Lambda\Delta\bar{V}$. Combining the objective function and (6), the optimization problem for the motion velocity constraint can be obtained as follows:

$$\begin{cases}J=\min\dfrac{1}{2}\Delta\bar{V}^TP\Delta V+b^T\Delta\bar{V}\\ \Theta_0\Delta V\le d\end{cases}\tag{7}$$

where $P=2(\Theta^T\Pi\Theta+\Lambda),b=2\Theta^T\Pi(\Gamma V(k-1)-\bar{X}_d)$, and Π and Λ are positive definite symmetric matrices with appropriate dimensions.

Using quadratic programming to solve (7), the velocity increment $\Delta\bar{V}(k)$ can be obtained. The prediction model in (4) can then be used to calculate $V(k)$ and obtain the velocity constraint of each wheel.

COMPENSATION TRACKING CONTROL

In the passive training stage, the controller can be designed using model (2) as follows:

$$u(t)=\hat{B}(\theta)M_a(\ddot{X}_d(t)-e_1(t)-e_2(t)-\hat{\xi}(t)).\tag{8}$$

Here $e_1(t)=X(t)-X_d(t),e_2(t)=V(t)-\dot{X}_d(t),V(t)$ is the limited motion velocity, $X_d(t)$ is the specified trajectory, and $\hat{\xi}(t)$ is the estimated human–robot uncertain environment, respectively.

The stability of the system can be achieved by establishing Lyapunov $V_v(t)=(1/2)e_1^T(t)e_1(t)+(1/2)e_2^T(t)e_2(t)+(1/2)$ $\tilde{\beta}^T\tilde{\beta}$, where $\tilde{\beta}=\beta-\hat{\beta}$ is the estimated error of the weight β. In the passive training stage, the main purpose of our design is to make the RRDS track the training trajectory specified by the doctor at a limited velocity and suppress uncertain motion environments to ensure the safety of the human–robot system.

After the passive training stage, the rehabilitee achieved a certain leg support strength. The RRDS design movement pattern must conform to the walking characteristics of the rehabilitee. The rehabilitee should express the desire to participate in the training process. Next, the RRDS function should be switched directly to the active training stage.

ACTIVE TRAINING

As the system enters the active training stage, the RRDS needs to identify the velocity of the rehabilitee to achieve the coordination of the human–robot velocity and stable tracking in a limited learning time to ensure the safety of the rehabilitee.

VELOCITY DECISION METHOD

In the active training process, the sensor was used to measure the walking velocity of the rehabilitee and compare it with the actual movement velocity of the RRDS. The reward and punishment value functions of the decision-making process were designed according to the difference in the compared velocity values. The action of the velocity decision ensures coordination between the human and robot velocities. The RRDS motion velocity decision states are described as $\text{state}_1, v_t < V_t$; $\text{state}_2, v_t = V_t$; and $\text{state}_3, v_t > V_t$.

Here v_t is the current velocity of the RRDS, V_t is the current velocity of the rehabilitee, and the velocity change value adjusted for each action by the RRDS is Δv. v_{t+1} is the velocity of the robot at the next moment, and the decision-making actions are described as $a_1, v_{t+1} = v_t + \Delta v$; $a_2, v_{t+1} = v_t$; and $a_3, v_{t+1} = v_t - \Delta v$.

Let $\Delta V = v_t - V_t$ represent the difference between the RRDS and velocity value of the rehabilitee at the current moment. The reward and punishment value function R is designed when $|\Delta V| \le \tau$, $R = 100$; $|\Delta V| > \tau$, and $R = 0$, where τ is the specified very small velocity difference value and $\tau \ge 0$. When $|\Delta V|$ is less than τ, the reward and punishment values are $R = 100$. Thus, the $|\Delta V|$ decreases until it reaches zero. At this time, the RRDS realizes the velocity decision of state_2. The steps of the RRDS motion velocity decision are as follows:

Step 1 is to initialize the behavior (S, A) of the RRDS, where S is the current state and A is the current action taken by the robot. Set the learning rate α of the robot update state, the decay coefficient γ, and selection probability ε of the decision-making action, where $\alpha \in [0,1], \gamma \in [0,1]$, and $\varepsilon \in [0,1]$.

Step 2 is to compare the current velocity values of the RRDS and rehabilitee; determine the state of the robot in state_1, state_2, and state_3; and denote this as S in each state. To determine the current moment behavior (S, A), the RRDS selects any action in a_1, a_2, and a_3 with probability ε and denotes it as A. Further, according to the reward and punishment values of R, the RRDS enters the next state and denotes it as S'. We then use probability ε to select a new action A' and obtain a new behavior (S', A'). According to the current moment reward and punishment value R for obtaining (S, A), the value Q(S, A) is updated as $Q(S,A) \leftarrow Q(S,A) + \alpha[R + \gamma Q(S',A') - Q(S,A)]$, and an action decision can be completed. Here $Q(S, A)$ is the value obtained by the current state behavior (S, A), and $Q(S', A')$ is the value of the state behavior (S', A') at the next moment.

By taking (S', A') as the current new state and action and repeating step 2, the RRDS continues to make action decisions until the velocity error meets $|\Delta V| \le \tau$, and the RRDS ensures that the human and robot velocities are coordinated by continuously adjusting the velocity.

> “IN THE ACTIVE TRAINING STAGE, SECONDARY INJURY OF THE REHABILITEE IS AVOIDED BECAUSE OF THE UNCOORDINATED HUMAN–ROBOT VELOCITY, ENSURING THE SAFETY OF THE REHABILITEE DURING THE TRAINING PROCESS.”

TIME-LIMITED LEARNING ITERATIVE TRACKING CONTROL

The kth learning iteration of the system model in (2) can be expressed as follows:

$$\ddot{X}_k(t) = M_a^{-1} B(\theta) u_k(t) + \xi_k(t). \quad (9)$$

For model (9), the time-limited learning iterative controller is designed as follows:

$$u_k(t) = \hat{B}(\theta) M_a (\ddot{x}_d(t) + \dot{\phi}(e_{1,k}(t)) - e_{1,k}(t) + \phi(z_k(t)) - \hat{\xi}_k(t)) \quad (10)$$

where $\hat{\xi}_k(t) = \hat{\xi}_{k-1}(t) - \vartheta z_k(t)$, the actual trajectory of kth learning is $X_k(t)$, and the desired trajectory is $X_d(t)$. Therefore, the kth learning errors can be constructed as $e_{1,k}(t) = X_k(t) - X_d(t)$, $z_k(t) = e_{2,k}(t) - \phi(e_{1,k}(t))$, $e_{2,k}(t) = \dot{X}_k(t) - V(t)$, $\phi(e_{1,k}(t)) = -R_1 Sig(e_{1,k}(t)))^{\varpi}$, and $\phi(z_k(t)) = -R_2 Sig(z_k(t))^{\varpi}$. $V(t)$ represents the determined motion velocity of the robot, and $\hat{\xi}_k(t)$ is the estimated value of $\xi(t)$ for the kth learning, where $\vartheta > 0$ is the learning gain.

By establishing the Lyapunov function $V_k(t) = (1/2) e_{1,k}^T(t) e_{1,k}(t) + (1/2) z_k^T(t) z_k(t) + (1/2) \tilde{\xi}_k^T(t) \tilde{\xi}_k(t)$, the system is stabilized within the limited learning time T, and $T \le (V_i^{1-\zeta}(e_{1,k}(0))) / (\bar{l}(1-\zeta))$, which suppresses the influence of human–robot uncertain environments on the tracking performance of the system, thus achieving the coordination of human–robot velocity.

In the active training stage, secondary injury of the rehabilitee is avoided because of the uncoordinated human–robot velocity, ensuring the safety of the rehabilitee during the training process. A block diagram of the proposed passive and active direct switching control systems for the RRDS is shown in Figure 4.

SIMULATION ANALYSIS

To verify the effectiveness of the proposed method, the performance of the RRDS is required to include the following: in the passive training stage, according to the training requirements, the velocity constraints specified by the doctor are listed as shown in Table 1; when $tf = 8$ s, the passive training is directly switched to the active training; in the active training stage, the velocity decision error constraints are listed as shown in Table 2; and in the entire whole training process, the trajectory tracking error constraints are listed as shown in Table 3. The tracking training for passive and active direct switching was performed on a motion trajectory specified by a doctor. The tracking trajectory was described as $x_d(t) = t + 2e^{-0.5t}$, $y_d(t) = t + 2e^{-0.5t}$, and $\theta_d(t) = \pi/4$. The physical parameters in the simulation study were $M = 58$ Kg, $m = 60$ Kg, $L = 0.4$ m, $I_0 = 27.7$ kg $\cdot$ m^2, and $r_0 = 0.4(1 + \text{rand}())$kg. The system initial value and

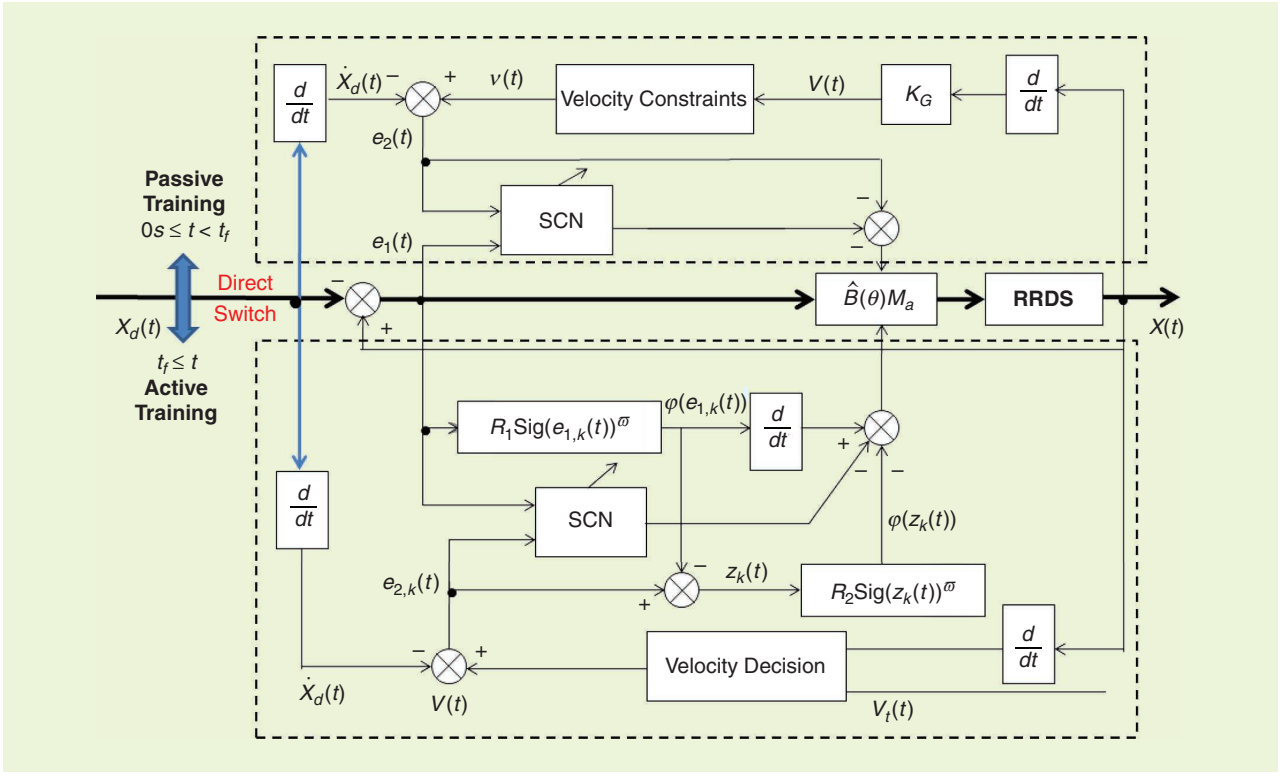

FIGURE 4. Block diagram of the proposed control system for the RRDS.

controller parameters of the RRDS are $x(0) = 2$ m, $y(0) = 2$ m, $\theta(0) = \pi/4$ rad, $v_x(0) = 0$ m/s, $v_y(0) = 0$ m/s, $v_\theta(0) - 0$ rad/s, $\upsilon = 6$, $R_1 = \text{diag}\{36, 45, 24\}$, and $R_2 = \text{diag}\{0.1, 5, 0.1\}$.

The simulation results are as follows:

Figure 5 shows the human–robot uncertain environments for the x-axis, y-axis, and rotation angle based on the SCN. The neural network accurately estimates the human–robot motion environments and lays a foundation for obtaining accurate tracking training. The trajectory and path tracking curves in the passive and active direct switching training process are shown in Figure 6(a)–(d). The RRDS suppresses the uncertain environments and achieves the switching training from passive to active at $t_f = 8$ s, whereas the trajectory errors on each axis realize $|e_{1x}(t)| \le 0.25$ m, $|e_{1y}(t)| \le 0.25$ m, and $|e_{1\theta}(t)| \le 0.25$ rad. Figure 6(e)–(g) shows the velocity tracking curves of the RRDS in the x-axis, y-axis, and rotation angle directions in the passive and active direct switching training process. It can be observed that the RRDS velocity is within the specified range of $|v_x(t)| \le 1$ m/s, $|v_y(t)| \le 1$ m/s, and $|v_\theta(t)| \le 0.25$ rad/s in the passive training stage, and as the walking ability of the rehabilitee increases, the system directly enters the active training stage, and the velocity decision errors of each axis satisfy $|\Delta V_x(t)| \le 0.03$ m/s, $|\Delta V_y(t)| \le 0.03$ m/s, and $|\Delta V_\theta(t)| \le 0.03$ rad/s. Moreover, the RRDS has the same safe movement velocity of the rehabilitee.

To verify the effectiveness of the proposed method for passive and active direct switching training, a simulation comparison was performed with [18], which proposed a random tracking control method for rehabilitation training robots. Considering the offset characteristics of the system's center of gravity and incomplete position output feedback information, the controller in [18] was used to track the training trajectory with passive and active direct switching training in this study. The simulation results are as follows:

TABLE 1. Velocity constraints.

$\lvert v_x(t)\rvert$	$\lvert v_y(t)\rvert$	$\lvert v_\theta(t)\rvert$
1 m/s	1 m/s	0.25 rad/s

TABLE 2. Velocity decision error constraints.

$\lvert \Delta v_x(t)\rvert$	$\lvert \Delta v_y(t)\rvert$	$\lvert \Delta v_\theta(t)\rvert$
0.03 m/s	0.03 m/s	0.03 rad/s

TABLE 3. Trajectory tracking errors constraints.

$\lvert e_{1x}(t)\rvert$	$\lvert e_{1y}(t)\rvert$	$\lvert e_{1\theta}(t)\rvert$
0.25 m	0.25 m	0.25 rad

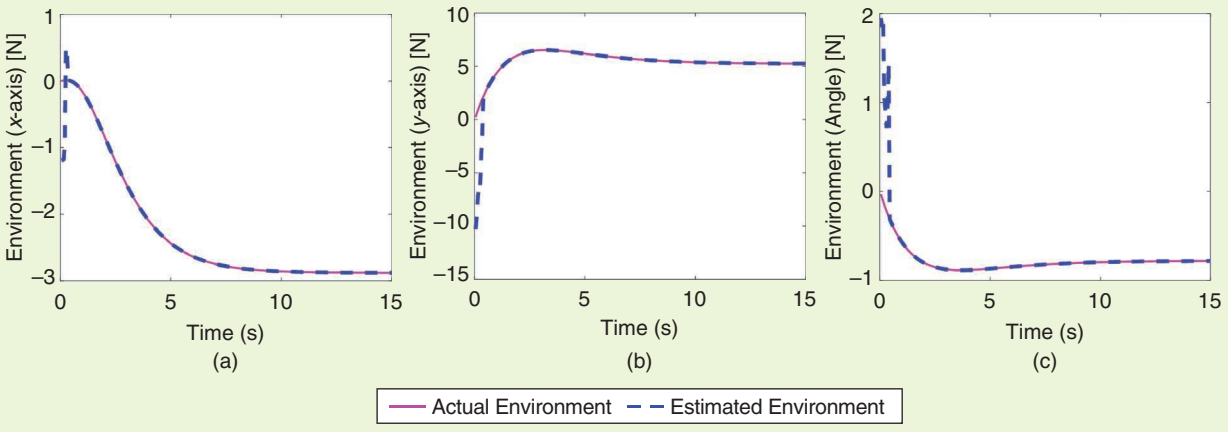

FIGURE 5. Human–robot uncertain environments of the RRDS for each motion axis. (a) Environment estimation of the *x*-axis. (b) Environment estimation of the *y*-axis. (c) Environment estimation of the angle.

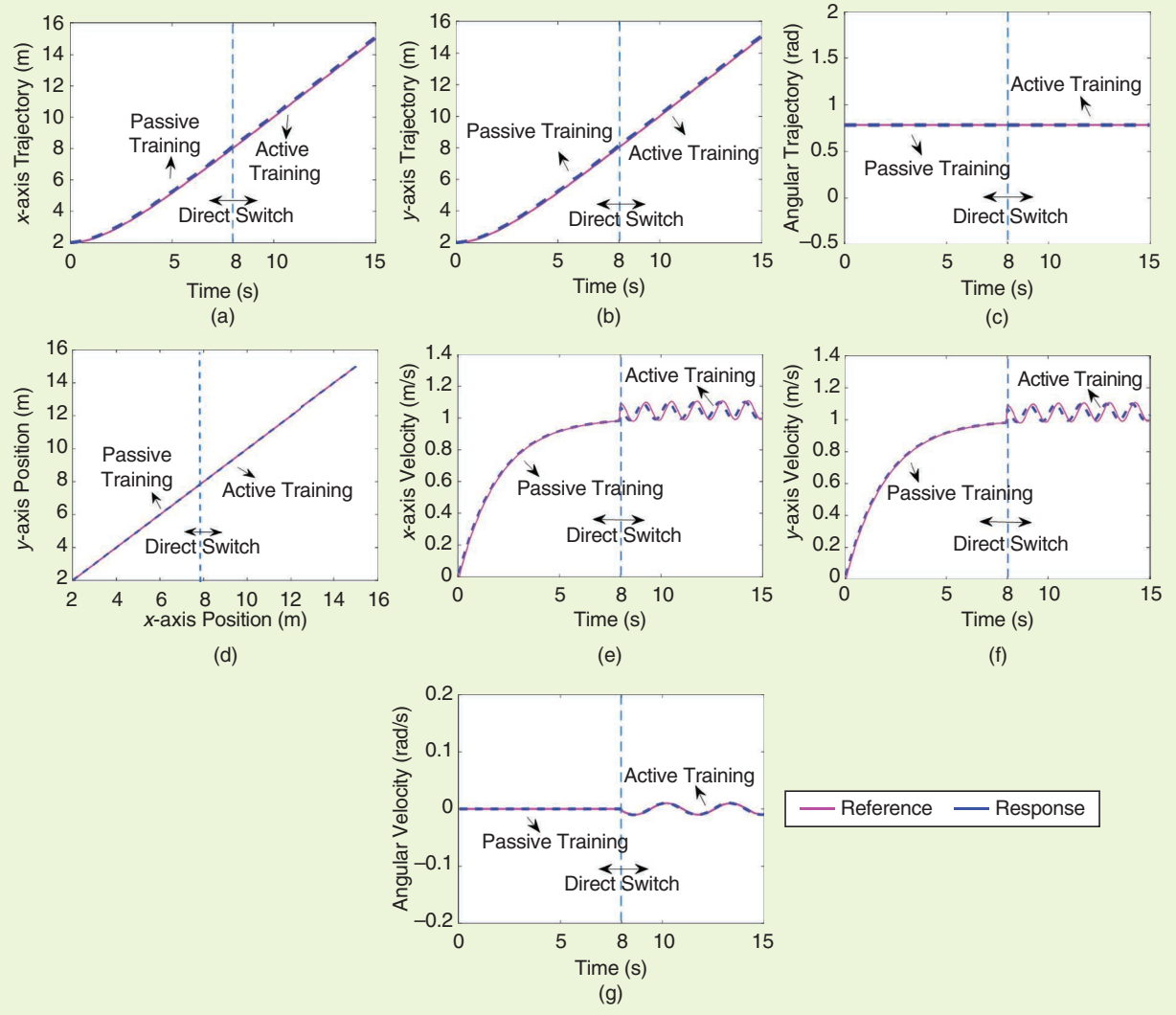

FIGURE 6. Path tracking of RRDS and velocity tracking curves of each motion axis (the method of this article). (a) Trajectory tracking of the *x*-axis. (b) Trajectory tracking of the *y*-axis. (c) Trajectory tracking of the angle. (d) Path tracking. (e) Velocity tracking of the *x*-axis. (f) Velocity tracking of the *y*-axis. (g) Velocity tracking of the angle.

Figure 7(a) shows the path tracking curves of the RRDS in the passive and active direct switching training system. It can be observed that the RRDS can achieve stable path tracking training. Moreover, the controller in [18] could suppress the impact of the system offset on the tracking performance. Figure 7(b)–(d) shows the velocity tracking curves of the RRDS in the passive and active direct switching training process. It can be observed that the robot in [18] could achieve velocity tracking in the passive training stage. However, in the active training stage, the velocity exhibited a large deviation and could not adapt to the velocity of the rehabilitee. Thus, the velocity coordination could not be realized between the human and the robot, which threatens the safety of rehabilitee. This shows that the controller of [18] cannot directly switch from passive to active training and that it can only make the rehabilitee walk in the passive mode for rehabilitation exercises.

The controller design method was applied to the model proposed in [19] to illustrate the superiority of the proposed method for passive and active direct switching motions. The tracking curve of the manipulator is the same as that of the model proposed in this study, and the simulation results are as follows.

Figure 8(a) shows the path tracking curves of the manipulator in the passive and active direct switching motions. It can be observed that the manipulator achieved stable tracking and that the controller could suppress uncertain motion environments. Figure 8(b) and (c) plots the angular velocity tracking curves of the joints and for the passive and active direct switching motions, respectively. It can be observed that the manipulator velocity was constrained within the specified range for passive motion. Moreover, for active motion, the manipulator had the capability of velocity decision. This shows that the designed controller can contribute to stable tracking in the manipulator for both passive and active direct switching motions and that it can improve the safety and intelligence of the system.

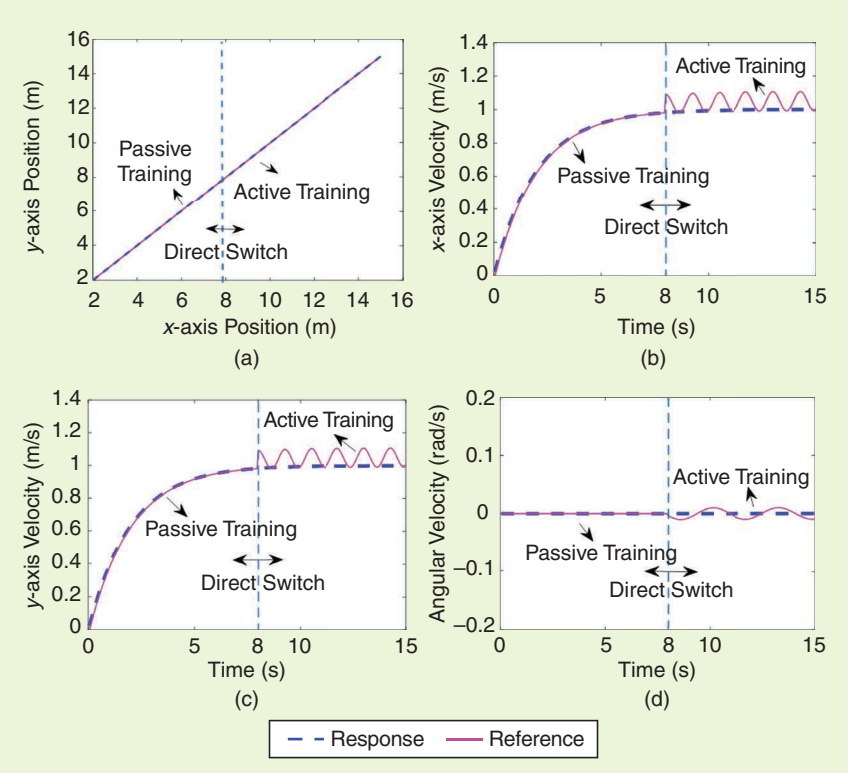

FIGURE 7. Path tracking of RRDS and velocity tracking curves of each motion axis [18]. (a) Path tracking. (b) Velocity tracking of the *x*-axis. (c) Velocity tracking of the *y*-axis. (d) Velocity tracking of the angle.

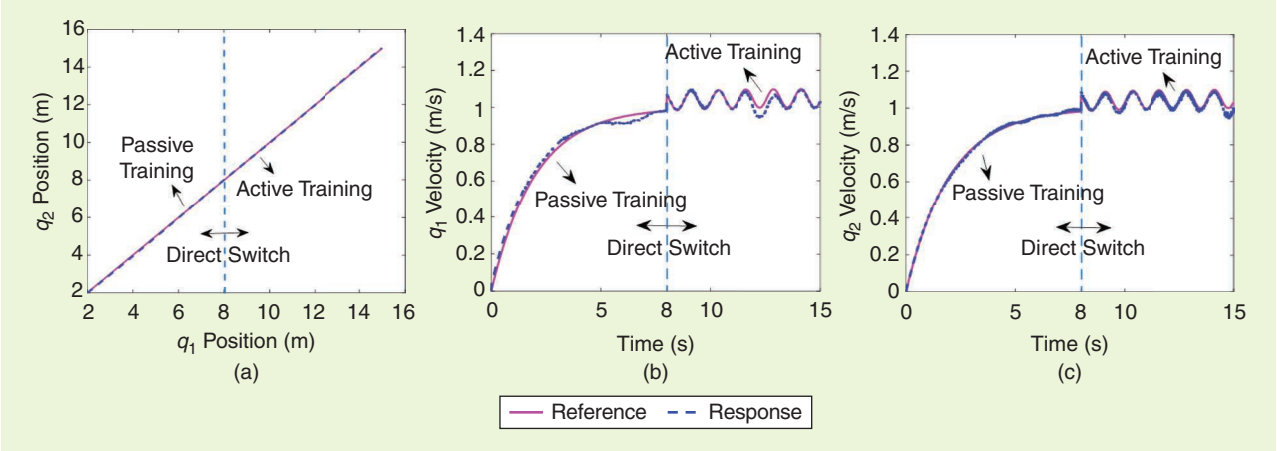

FIGURE 8. Path tracking of manipulator and velocity tracking of the double joint. (a) Path tracking. (b) Velocity tracking of q_1. (c) Velocity tracking of q_2.

TABLE 4. Rehabilitation training evaluation results.

QUADRICEPS FEMORIS	GLUTEUS MEDIUS	ILIOPSOAS MUSCLE	WALKING ABILITY
107% up	173% up	137% up	127% up

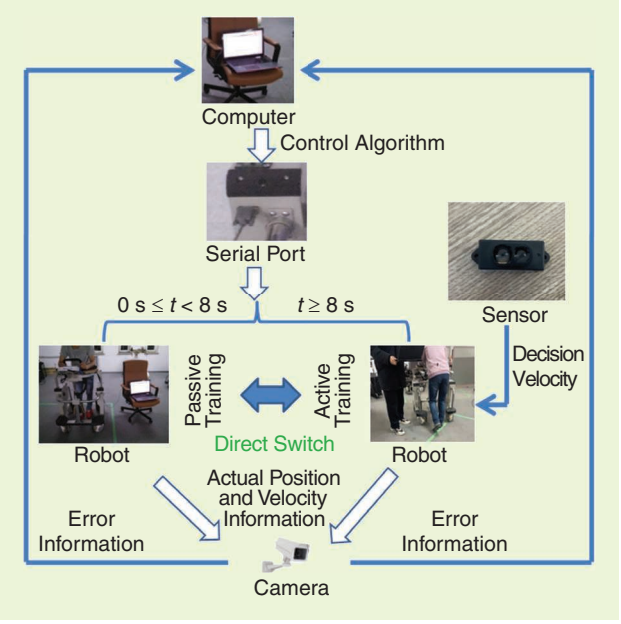

FIGURE 9. Experimental environment.

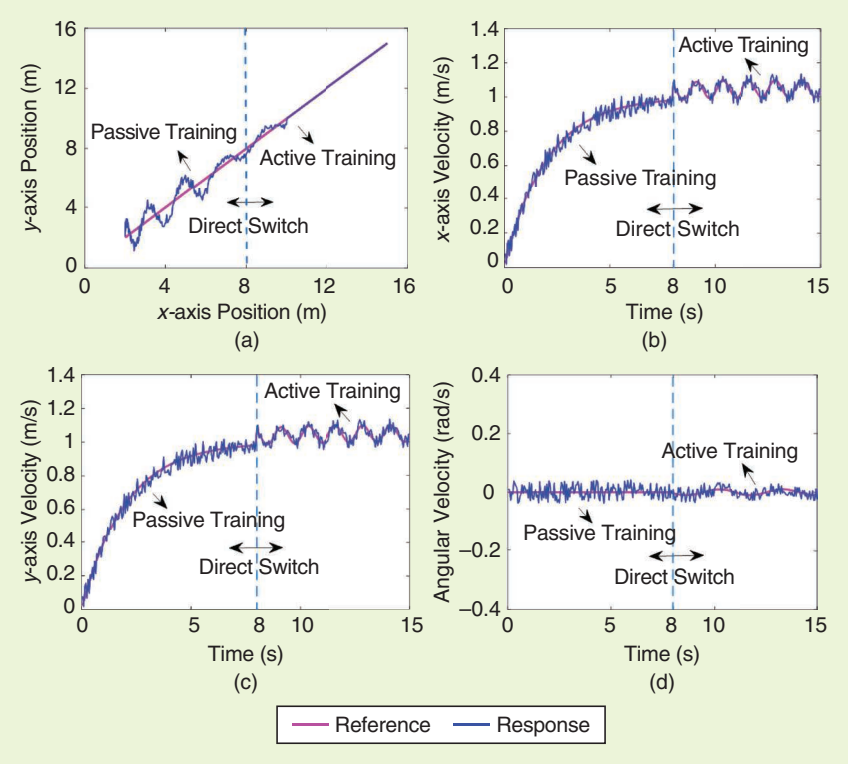

FIGURE 10. Path tracking of RRDS and velocity tracking curves of each motion axis. (a) Path tracking. (b) Velocity tracking of the *x*-axis. (c) Velocity tracking of the *y*-axis. (d) Velocity tracking of the angle.

EXPERIMENTAL RESULTS

To verify the superiority of the proposed passive and active direct switching training in this study, an experimental study of the RRDS was performed. Infrared sensors were used to measure the active walking velocity during rehabilitation and compare it with the actual movement velocity of the RRDS. The robot then determined its velocity and stored it.

In our earlier work, we conducted an experimental study on passive training mode of the RRDS for nine elderly rehabilitees with lower-limb walking disorders, aged 78 to 92 [20]. The rehabilitee's ability to walk and the strength of their lower limbs significantly improved after 4.5 months of rehabilitation training, which they underwent five times per week for five minutes each (Table 4).

In the current experiment, the training objects were extended to graduate students with normal walking ability to test the performance of the new RRDS training mode, including the passive training velocity constraints, direct switching between passive and active training, and active training velocity decision function. The motion path of the RRDS adopted the same linear path as in the simulation analysis. The initial motion position and velocity, passive and active direct switching control methods, and learning times were the same as those in the simulation. The experimental process is illustrated in Figure 9.

As shown in Figure 9, the walking ability during the initial rehabilitation was weak during the training process of the robot. The robot needs to track the path specified by the doctor, and the rehabilitee enters the passive training stage. The RRDS performs the algorithm of compensation control with velocity constraints through the serial port and collects the position and velocity information from the camera. According to the tracking error, the controller continuously corrects the motion trajectory and velocity of the RRDS, restrains the impacts of uncertain environments on the robot's tracking performance, and restricts the velocity within a specified range to ensure the safe training of the rehabilitee. When the passive training stage reaches a certain amount of time, with an increase in the walking ability, the rehabilitee can participate in active exercises. In this case, the RRDS directly switches from passive to active training. The physical and controller parameters of the RRDS are the same as those of the simulation values, and the experimental results are as follows.

Figure 10(a) shows the path tracking curve of the RRDS in the experiment. It can be observed that the motion path of the robot fluctuated slightly at the beginning. However, it met the allowable error range of the human–robot system. As the number of learning times increased, the tracking error gradually decreased, and the RRDS finally achieved stable tracking for both passive and active direct switching training. Figure 10(b)–(d) shows the velocity tracking curves in the passive and active switching training process. From these figures, it can be observed that the RRDS velocity constraint range of each axis satisfied $|v_x(t)| \leq 1$ m/s, $|v_y(t)| \leq 1$ m/s, and $|v_\theta(t)| \leq 0.25$ rad/s in the passive training stage. With the improvement of the walking ability, the RRDS directly switched to the active training stage at $t_f = 8$ s. Moreover, the velocity was constantly adjusted to satisfy the decision errors on each axis within the range of $|\Delta V_x(t)| \leq 0.03$ m/s, $|\Delta V_y(t)| \leq 0.03$ m/s, and $|\Delta V_\theta(t)| \leq 0.03$ rad/s. The experimental results showed that the proposed passive and active direct switching training improves the intelligence and security of the RRDS.

CONCLUSIONS

This article presented the development of the RRDS, which is an intelligent rehabilitation robot with passive and active direct switching training. Compared to other rehabilitation robots, the RRDS has the following intelligent features: 1) it can directly switch from passive training to active training; 2) during passive training, the velocity of the robot is limited to a safe range, which improves the safety of the human–robot system; and 3) during active training, the velocities of the robot and rehabilitee are maintained in harmony, which improves the intelligence of the system. The safety of the RRDS was guaranteed by its structure and training processes. In terms of structure, the functions of each part of the robot provide convenience and safety for the rehabilitee during training. Passive and active direct switching training is possible during the training processes. The human–robot velocity is restricted within the safe range during passive training. When passive training is directly switched to active training, the human–robot velocity remains consistent, and the system realizes stable tracking in a limited learning time. The performance of the RRDS was experimentally verified.

ACKNOWLEDGMENT

This work was supported by JSPSKAKENHI under Grant 15H03951, the CANON Foundation, the CASIO Science Promotion Foundation, and the Basic Research Program of the Education Department Foundation of Liaoning Province under Grant LJGD2019017.

AUTHORS

Ping Sun, School of Artificial Intelligence, Shenyang University of Technology, Shenyang 110870, P. R. China. Email: tonglongsun@sut.edu.cn.

Rui Shan, School of Artificial Intelligence, Shenyang University of Technology, Shenyang 110870, P. R. China. Email: shanrui123@163.com.

Shuoyu Wang, Department of Intelligent Mechanical Systems Engineering, Kochi University of Technology, Kochi 7828502, Japan. Email: wang.shuoyu@kochi-tech.ac.jp.

REFERENCES

[1] J. Cao, S. Q. Xie, and R. Das, "MIMO sliding controller for gait exoskeleton driven by pneumatic muscles," *IEEE Trans. Control Syst. Technol.*, vol. 26, no. 1, pp. 1–8, Jan. 2018, doi: 10.1109/TCST.2017.2654424.

[2] P. K. Jamwal et al., "Impedance control of an intrinsically compliant parallel ankle rehabilitation robot," *IEEE Trans. Ind. Electron.*, vol. 63, no. 6, pp. 3638–3647, Jun. 2016, doi: 10.1109/TIE.2016.2521600.

[3] X. Li et al., "BEAR-H: An intelligent bilateral exoskeletal assistive robot for smart rehabilitation," *IEEE Robot. Autom. Mag.*, vol. 29, no. 3, pp. 34–46, Sep. 2022, doi: 10.1109/MRA.2021.3129451.

[4] G. Masengo et al., "A design of lower limb rehabilitation robot and its control for passive training," in *Proc. 10th IEEE Int. Conf. Cyber Technol. Autom., Control, Intell. Syst.*, 2020, pp. 152–157, doi: 10.1109/CYBER50695.2020.9278952.

[5] J. Chen, "Design and passive training control of elbow rehabilitation robot," *Electronics*, vol. 10, no. 10, 2021, Art. no. 1147, doi: 10.3390/electronics10101147.

[6] X. F. Zeng et al., "Reviewing clinical effectiveness of active training strategies of platform-based ankle rehabilitation robots," *J. Healthcare Eng.*, vol. 2018, pp. 1–13, Feb. 2018, doi: 10.1155/2018/2858294.

[7] P. Stegall, D. Zanotto, and S. K. Agrawal, "Variable damping force tunnel for gait training using ALEX III," *IEEE Robot. Autom. Lett.*, vol. 2, no. 3, pp. 1495–1501, Jul. 2017, doi: 10.1109/LRA.2017.2671374.

[8] T. Ohnuma, G. Lee, and N. Y. Chong, "Particle filter based feedback control of JAIST active robotic walker," in *Proc. IEEE Int. Symp. Robot Human Interactive Commun.*, 2011, pp. 264–269, doi: 10.1109/ROMAN.2011.6005262.

[9] J. Y. Kim, J. J. Kim, and K. Park, "Gait training algorithm of an end-effector typed hybrid walking rehabilitation robot," *Int. J. Precis. Eng. Manuf.*, vol. 20, no. 10, pp. 1767–1775, 2019, doi: 10.1007/s12541-019-00185-y.

[10] J. Y. Kim et al., "Development and evaluation of hybrid walking rehabilitation robot DDgo pro," *Int. J. Precis. Eng. Manuf.,* vol. 21, no. 11, pp. 2105–2115, 2020, doi: 10.1007/s12541-020-00404-x.

[11] "Gait and Balance." Hocoma. Accessed: Sep. 10, 2022. [Online]. Available: https://www.hocoma.com/solutions/gait-balance/

[12] "What's Hal?" Cyberdyne. Accessed: Sep. 10, 2022. [Online]. Available: https://www.cyberdyne.jp/english/products/HAL/index.html

[13] Z. H. Dong, J. V. Luces, and Y. Hirata, "Control and evaluation of body weight support walker for overground gait training," *IEEE Robot. Autom. Lett.*, vol. 6, no. 3, pp. 4632–4639, Jul. 2021, doi: 10.1109/LRA.2021.3068691.

[14] Q. Liu et al., "Fuzzy sliding control of a multi-DOF parallel robot in rehabilitation environment," *Int. J. Humanoid Robot.*, vol. 11, no. 1, pp. 1223–1251, 2014, doi: 10.1142/S0219843614500042.

[15] W. Meng et al., "Robust iterative feedback tuning control of a compliant rehabilitation robot for repetitive ankle training," *IEEE/ASME Trans. Mechatronics*, vol. 22, no. 1, pp. 173–184, Feb. 2017, doi: 10.1109/TMECH.2016.2618771.

[16] W. He et al., "Neural network control of a rehabilitation robot by state and output feedback," *J. Intell. Robot. Syst.*, vol. 80, no. 1, pp. 15–31, 2015, doi: 10.1007/s10846-014-0150-6.

[17] P. Sun, S. Y. Wang, and H. B. Chang, "Tracking control and identification of interaction forces for a rehabilitative training walker whose centre of gravity randomly shifts," *Int. J. Control*, vol. 94, no. 5, pp. 1143–1155, 2021, doi: 10.1080/00207179.2019.1635271.

[18] H. B. Chang, P. Sun, and S. Y. Wang, "Output tracking control for an omnidirectional rehabilitative training walker with incomplete measurements and random parameters," *Int. J. Syst. Sci.*, vol. 48, no. 12, pp. 2509–2521, 2017, doi: 10.1080/00207721.2017.1324064.

[19] A. Tayebi, "Adaptive iterative learning control for robot manipulators," *Automatica*, vol. 40, no. 7, pp. 1195–1203, 2004, doi: 10.1016/j.automatica.2004.01.026.

[20] Y. S. Wang et al., "Developing the omni-directional mobile walker and verifying its effect of increase in the muscle power," (in Japanese), in *Proc. JSME Symp. Welfare Eng.*, 2007, vol. 2007, pp. 176–177, doi: 10.1299/jsmewes.2007.176.